JOURNAL OF OPTOELECTRONICS AND ADVANCED MATERIALS Vol. 9, No. 5, May 2007, p. 1273 - 1276

Characterization of ZnTe homo-epitaxial layers by means of synchrotron X-ray topography

K. MIZUNO*, H. OKAMOTO[a], P. PRETE[b], N. LOVERGINE[c]
Dept. of Material Science, Shimane Univ., Matsue, 690-8504, Japan
[a]Dept. of Health Science, Kanazawa Univ., Kanazawa 920-0942, Japan
[b]IMM-CNR, Sez. di Lecce, Via Arnesano, I-73100 Lecce, Italy
[c]Dept. of Innovation Engineering, Univ. of Lecce, Via Arnesano, I-73100 Lecce, Italy

Synchrotron X-ray reflection topography was used to evaluate the crystal quality of a ZnTe epilayer grown by MOVPE on a low dislocation density (111) ZnTe substrate. The epilayer thicknesses were 0.35 μm and 3.0 μm, and the growth temperature was 325°C or 350°C. Another specimen whose epilayer was grown at 400°C with 3.0 μm thickness had a 0.35 μm thick buffer layer grown at 325°C. Reflection topographs and rocking curves were recorded from four equivalent 224 reflections using an X-ray wavelength of 0.1578 nm. Topographs of specimens with the epilayer grown at 325°C and 350°C did not show images of line defects, such as misfit dislocations. However, we could observe line images in the specimen with the epilayer grown at 400°C and with the buffer layer grown at 325°C. The line images were not observed in transmitted X-ray Laue topographs using a white X-ray beam. Therefore, it was concluded that the line defects existed in the epilayer and not the substrate. In addition, topographs taken with other diffraction planes showed the same images except for reversed image contrast. Therefore, the defects did not have characteristic strain fields such as for dislocations, and they are stacking faults grown in the epilayer during high temperature growth.

(Received November 14, 2006; accepted April 12, 2007)

Keywords: ZnTe, homo-epitaxial thin layer, Synchrotron X-ray topography

1. Introduction

Considerable efforts have been applied towards applications of wide band-gap II-ε compound semiconductors, such as ZnSe and ZnCdSe alloys, for realizing high efficiency light emitting diodes (LEDs) and laser diodes (LDs) operating in the blue-green region. [1] Among the II-ε semiconductors, ZnTe has a direct transition band structure with a 2.26 eV band-gap, and is a promising material for realizing high brightness LEDs and LDs operating in the green spectral range of light. Unfortunately, until now, the lack of II-ε single crystal substrates with low lattice defect densities, and difficulty in *p*-type doping of most wide gap II-ε compounds, have prevented the fabrication of long lifetime LEDs and LDs. In the past, epitaxial growth of II-ε based devices has been attempted on GaAs substrates. However, chemical, lattice and thermal mismatch between II-ε epilayers and GaAs have resulted in residual lattice strains and interface defects, limiting device performance. [2,3].

In the case of ZnTe-based devices, substrate limitations have recently been overcome, and high crystalline quality ZnTe wafers obtained by the vertical gradient freezing (VGF) method [4,5] have become available, allowing for homoepitaxy of good structural and optical quality ZnTe by both molecular beam (MBE) [6] and metalorganic vapor phase (MOVPE) epitaxy. [7] Moreover, *n*-type ZnTe:Al homoepitaxial layers were demonstrated using MBE. [8] This opened the path to the realization of ZnTe-based vertical *p-i-n* diode structures.[9,10]. The growth of ZnTe-based devices on ZnTe substrates thus has significant technological potential for applications in signal transmission (at around 560 nm) through optical fibers, as alternatives to both low quantum efficiency GaP- and complex InGaN-based green LEDs and LDs.

Within this scenario, it is of primary importance to further optimize the growth of ZnTe homoepitaxial layers by studying their microstructural characteristics. We have therefore examined the lattice perfection in the ZnTe homoepitaxial layer using synchrotron X-ray reflection topography.

2. Experimental procedure

Homoepitaxial ZnTe layers were deposited on a (001) ZnTe substrate by atmospheric pressure MOVPE using dimethylzinc (Me_2Zn) and di-isopropyltellueide ($^iPr_2Te$) as Zn and Te precursors, respectively. [7,11] The substrates were cleaved from P doped ZnTe wafers supplied by Nikko Metals Co., Ltd. of Japan. In order to eliminate any oxides or contamination from the surface for ZnTe epitaxy, the as-received substrates were carefully cleaned and etched as described previously. [7] The substrates were then heat-treated in the MOPVE reactor under a 1.0 l/min H_2 flow at 350 °C immediately before epilayer growth. [11] The epilayer thicknesses were 0.35 μm and 3.0 μm, and the growth temperature was 325°C or 350°C. Another specimen, with an epilayer grown at 400°C with a 3.0 μm thickness, had a 0.35 μm thick buffer layer grown at 325°C. The epilayer growth conditions and the sample names are

summarized in Table 1. The Te:Zn precursors molar flow ratio in the vapor was maintained constant at 1:1.

Table 1. Sample names, growth conditions and thickness of the epitaxial layer. Only the ZT256 sample had a buffer layer.

	Epilayer		Buffer layer	
Sample name	Thickness (μm)	Growth temperature (°C)	Thickness (μm)	Growth temperature (°C)
ZT225	3	225	-	-
ZT226	3	250	-	-
ZT250	0.35	250	-	-
ZT256	3	400	0.35	325

We carried out topographic observations at the Photon Factory (PF), located in the High Energy Accelerator Research Organization (KEK), Japan. Reflection topographs were obtained at the experiment station for precision diffraction, BL-15C, using a specimen with dimensions of approximately 10 × 20 × 0.4 mm. A 224 asymmetric reflection topograph was obtained at an X-ray wavelength of 0.1578 nm. Fig. 1 shows the schematic experimental arrangement of the X-ray reflection topography. With the synchrotron operating at 2.5 GeV and ~300 mA, the typical exposure time was 7 min. All the topographs were recorded on Ilford L-4 Nuclear Plates with a 25-μm-thick emulsion.

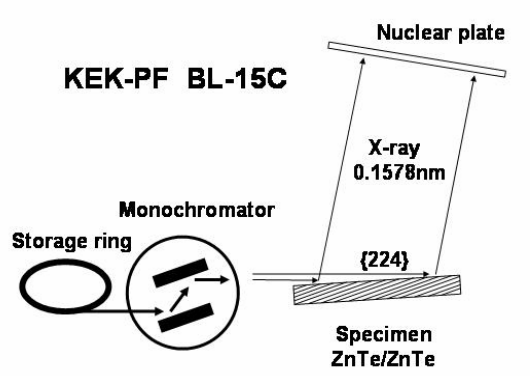

Fig. 1. Schematic diagram of the beam line and the experimental set-up for X-ray reflection topography used in this study.

3. Results and discussion

Fig. 2 shows normalized X-ray rocking curves of the ZT225 sample with the (2-24) reflection measured under the same condition of taking topographs. All the rocking curves showed ill-shaped curves with divided peaks, as shown in Fig. 2. The peaks of the rocking curves of all the specimens were split into 2 or 3 small sub-peaks. We therefore took topographs at each sub-peak and composed each topograph for observation of the entire area of the specimen. Topographs taken at each sub-peak indicated by the arrows in Fig. 2 are shown in Fig. 3. Figure 3 (a) and (b) shows the topographs taken at the low angle- and high angle-side sub-peaks in Fig. 2. Each topograph in Fig. 3 shows a different area of the epilayer sample in spite of the same diffraction conditions (almost) being used in both cases. This indicates that the crystal plane in the epilayer is bent, since almost the entire area of the epilayer does not satisfy the Bragg condition. Thus, improvements in the crystal perfection in the ZnTe wafer are still necessary. Therefore, we composed each topograph so as to observe the whole area of the sample. Figure 4 shows the topographs of the ZT225 sample with (2-24) and (224) reflections. There are many line images originating from scratches and shadows of the surface dust. However, images of defects such as dislocations could not be observed in the topographs in Fig. 4. Fig. 5 shows the composed topographs of ZT226 and ZT250 samples with the (2-24) reflection. In the ZT250 topograph, we can observe several curved lines similar to contour lines. These lines may have originated in the deviation of the thickness of the epilayer since the thickness of the sample at 0.35 μm is very thin. The composed reflection topographs of the ZT226 sample with a buffer layer are shown in fig. 6. A number of line images are observed in the topographs in contrast with the above results. An observable boundary line among the pre-composed topographs is indicated by an arrow in Fig. 6. Although the topographs were taken with other diffraction planes, there is no remarkable difference in the image pattern in Fig. 6(a) and (b). However, it can be clearly seen that the contrast of the line images is reversed between Fig. 6(a) and (b). In addition, the defect images consist of a white or black single line, and not a double line consisting of white and black lines. Usually, misfit-dislocation lines show white and black double lines due to the characteristic strain field in the reflection topograph.

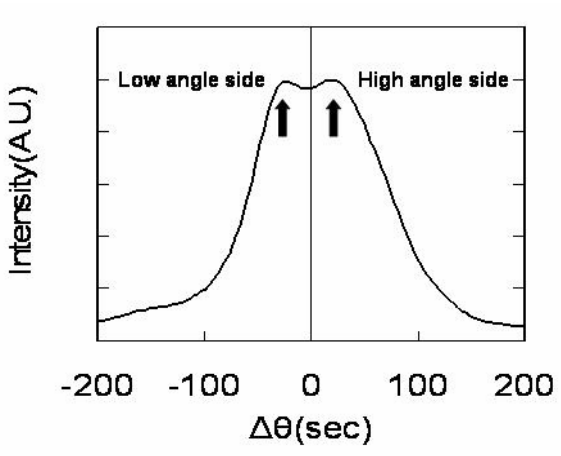

Fig. 2. Rocking curve of the ZnTe epilayer sample (ZT225) with 224 reflections. The rocking curves showed an ill-shaped rocking curve. The peak of the curve consists of 2 small sub-peaks indicated by arrows.

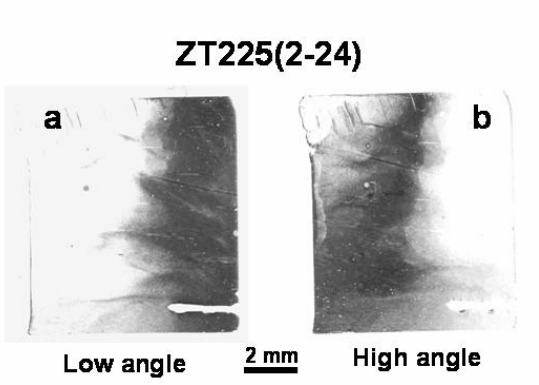

Fig. 3. Topographs taken at each sub-peak indicated by arrows in Fig. 2. Panels (a) and (b) are the low angle-side and high angle-side sub-peak image of the rocking curve, respectively. Each topograph shows a different area image of the epilayer sample although almost the same diffraction conditions was used.

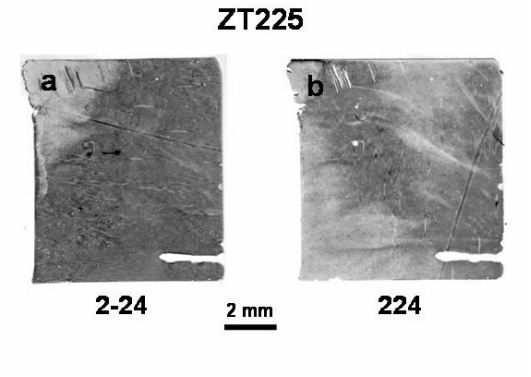

Fig. 4. Composed topographs of the ZT225 sample with (a) (2-24) and (b) (224) reflections. There are a number of line images originating from the scratches and shadows of the surface dust. However, images of defects such as dislocations could not be observed.

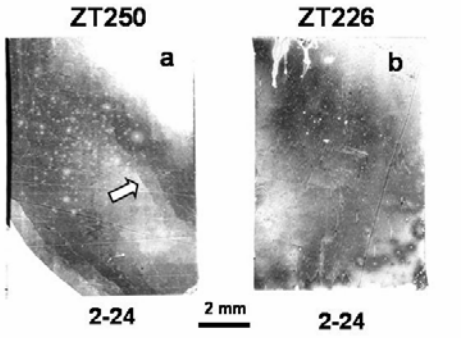

Fig. 5. Composed topographs of (a) ZT226 and (b) ZT250 samples with the (2-24) reflection. There are no line images originating from defects as similar as in Fig. 4.

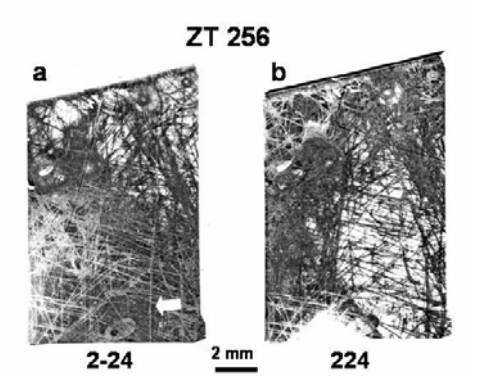

Fig. 6. Composed reflection topographs of the ZT256 sample with a buffer layer. Panels (a) and (b) are topographs with (2-24) and (224) reflections, respectively. An observable boundary line among pre-composed topographs is indicated by an arrow. Although the topographs were taken with the difference diffraction plane, there is no remarkable difference in the image pattern in (a) and (b). However, it can be clearly seen that the contrast of the line images is reversed between (a) and (b). These images did not have a characteristic strain field as for dislocations.

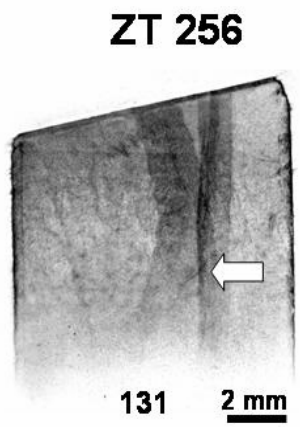

Fig. 7. Transmitted Laue topograph of the ZT256 sample. This shows the planar defect image indicated by an arrow, but does not show the line image observed in Fig. 6. Therefore, the line defect is located in the epitaxial layer and not the substrate. A boundary line between each reflection topograph taken by sub-peaks in the rocking curve corresponds to the edge of the planar defect image.

We also used the synchrotron white X-rays at the topographic station, BL-15B1, in the KEK-PF for identification of the line defects in Fig. 6. The transmitted Laue topograph is shown in Fig. 7. The diffraction plane was (131) and the wavelength of diffracted X-rays was 0.042 nm. This topograph shows the planar defect image, indicated by the arrow, but does not show the line image observed in Fig. 6. Therefore, the line defect is located in the epitaxial

layer and not in the substrate. A boundary line between each reflection topograph obtained by the sub-peaks in the rocking curve corresponds to the edge of the planar defect image. Di Luccio *et al*. have previously reported that a stacking fault was generated in the ZnTe epilayer grown at 400 ºC using an X-ray diffuse scattering experiment. [12]. Therefore, the line defect observed by the reflection topographs in this study is deduced to be a stacking fault.

4. Conclusions

We characterized the lattice perfection in a ZnTe homoepitaxial layer grown by MOPVE using synchrotron X-ray topography. There is a remarkable difference between ZnTe epilayers grown at 350 °C and 400 °C, and line images of stacking faults were observed in the epilayer sample grown at the higher temperature.

Acknowledgments

This work has been performed under the approval of the Photon Factory Advisory Committee (Proposal No. 2004G254).

References

[1] S. Itoh, K. Nakano, A. Ishibashi, J. Cryst. Growth **214/215**, 1029 (2000).

[2] M. Adachi, Z. M. Aung, K. Minami, K. Koizumi, M. Watanabe, S. Kuwamoto, T.Yamaguchi, H. Kasada, T. Abe, K. Ando, K. Nakano, A.Ishibashi, S. Itoh, J. Cryst. Growth **214/215**, 1035 (2000).

[3] N. Lovergine, F. Liaci, J.-D. Ganière, G. Leo, A. V. Drigo, F. Romanato,A. M. Mancini, L. Vasanelli, J. Appl. Phys. **78**, 229 (1995).

[4] K. Sato, M. Hanafusa, A. Noda, A. Arakawa, M. Uchida, T. Asahi, O.Oda, J. Cryst. Growth **214/215**, 1080 (2000).

[5] A. Arakawa, T. Asahi, K. Sato, Phys. Status Solidi B **229**, 11 (2002).

[6] J. H. Chang, M. W. Cho, H. M. Wang, H. Wenisch, T. Hanada, T. Yao, K.Sato, O. Oda, Appl. Phys. Lett. **77**, 1256 (2000).

[7] N. Lovergine, M. Traversa, P. Prete, K. Yoshino, M. Ozeki, M. Pentimalli, L. Tapfer, A. M. Mancini, J. Cryst. Growth **248**, 37 (2003).

[8] J. H. Chang, T. Takai, B. H. Koo, J. S. Song, T. Handa, T. Yao, Appl.Phys. Lett. **79**, 785 (2001).

[9] K. Kishino, I. Nomura, Y. Ochiai and S. B. Che, Phys. Status Solidi B**229**, 991(2002).

[10] A. Ueta, D. Hommel, Phys. Status Solidi A **192**, 177 (2002).

[11] M. Traversa, N. Lovergine, P. Prete, K. Yoshino, T. Di Luccio, G. Scalia,M. Pentimalli, L. Tapfer, P. Morales, A. M. Mancini, J. Appl. Phys. **96**, 1230 (2004).

*Corresponding author: mizuno@riko.shimane-u.ac.jp